Asia-Pacific Conference on FRP in Structures (APFIS 2007)
S.T. Smith (ed)

FLEXURAL BONDING CHARACTERISTICS OF NEWLY-DEVELOPED GFRP REBAR

H.S. Oh [1], J.S. Sim [2], M.K. Ju [2*] and T.S. Kang [2]

[1] *Jinju National University, South Korea*
[2] *Hanyang University, South Korea.*
Sa1-dong, Ansan-si, Kyungki-do, South Korea, 425-791. Email: mkju@hanyang.ac.kr

ABSTRACT

Nowadays, glass fiber reinforced polymer (GFRP) rebar has been received lots of attention as an alternate reinforcing material to the concrete structure. The bond capacity between concrete and reinforcing bars is one of the main characteristic of reinforced concrete structures. To evaluate the bonding characteristic of the GFRP rebar, one-way pull-out test have been performed by many researchers. But this kind of research may not be reasonable to investigate the flexural bonding performance for serviceability of the concrete flexural member reinforced with the GFRP rebar. In this study, the flexural bond strength of beam reinforced with the newly-developed GFRP rebar was evaluated under 4-point static and fatigue bending. For the flexural bonding test, the British Standard for flexural bonding was applied. This shape was fabricated to have concrete compressive block and semi-circle hollow with the GFRP rebar at the middle section of beam. It can simulate the ultimate state condition for reinforced concrete structure for bending. The variables were made to have bonding length of 5times ($5d_b$), 10times ($10d_b$) and 15times ($15d_b$) of the nominal diameter of GFRP rebar and the relationship between the bonding strength and the slip was analyzed.

In the result of test, two failure patterns were investigated. For static test, pull-out failure pattern was dominant in the $5d_b$ specimen and concrete tensile failure pattern was appeared in the $15d_b$ specimen. In the result of fatigue test, the number of loading cycle was decreased as the stress level was increased until failure. And also, as the embedment length was increased, the number of loading cycle was increased too. For the S-N relationship, the fatigue limit of the GFRP rebar was found to be around of the stress level of 70%. From these test results, the fatigue life was suggested as linear equation based on the Miner's theory by applying regression procedures with the fatigue test results. Flexural bonding characteristic of GFRP rebar be able to be adapted for GFRP rebar design and analysis to the concrete structure.

KEYWORDS

GFRP rebar, Static and fatigue bonding, Pull-out and Concrete tensile failure, S-N relationship

INTRODUCTION

In the vast majority of reinforced concrete applications, steel bar continues to be the most effective reinforcing material. But deterioration of steel reinforcement in concrete in a major factor in the deterioration of concrete structures. For this reason, glass fiber reinforced polymer (GFRP) rebar has been studied as an alternate reinforcing material to the concrete structure. Many researchers have studied one-way pull-out test for investigating the bonding characteristics of the FRP rebar. Malvar(1994) performed the bonding test with the GFRP rebar which has various surface types. Then he suggested the bonding model of the GFRP rebar. Focacci(2004), Consenza et al.(1995) and Eligehausen et al.(1983) applied the bonding model for steel rebar to the GFRP rebar and modified the bonding model for GFRP rebar. This kind of study, however, may not be suitable to the reinforced concrete structure mainly subjected to the flexural behavior. Tighiouart et al.(1998) investigated the flexural bonding capacity by fabricating the specimen which has concrete compressive block supported by pin. He evaluated the bonding strength by applying the ultimate equilibrium theory for the cross section then investigated the flexural bonding strength-slip relationship. In this study, the flexural bond strength of beam reinforced with the newly-developed GFRP rebar was evaluated under 4-point static and fatigue bending. For the flexural bonding test, the British Standard for flexural bonding was applied. This shape was fabricated to have concrete compressive block and semi-circle hollow with the GFRP rebar at the middle section of beam. It can simulate the ultimate state condition for reinforced concrete structure for bending. The variables were made to have bonding length of 5times ($5d_b$), 10times ($10d_b$) and 15times ($15d_b$) of the nominal diameter of GFRP rebar and the relationship between the bonding strength and the slip was analyzed.

EXPERIMENTAL PROGRAM

Experimental Variables

In this study, the newly-developed GFRP rebar which was manufactured by using pultrusion process in Korea was considered for evaluating the flexural bonding capacity. They were made of continuous longitudinal glass fiber strands bound together with a thermosetting epoxy. Figure 1 shows the GFRP rebar developed in this study. The rebar contain approximately 65% of glass fibers 35% of epoxy resin by volume. The surface treatment greatly improves bonding to concrete. To improve the bond between GFRP rebar and concrete, ribs similar to those of steel rebar were attached to a bare circular bar using a press molding process after pultrusion of the core section.

The rib section was a mixture of epoxy resin and fiberglass milled fibers. The rib used in the deformed GFRP rebar was a mixture of epoxy resin and milled glass fibers. The width and height of rib is 0.1mm and 0.2mm, respectively. The main GFRP matrix of glass fibers and epoxy resin, which resisted and the tensile stress. All rebars had a design tensile strength and modulus of elasticity of 616MPa and 42.5GPa, respectively.

Figure 2 shows the experimental variables in this study. The dimension of the test beam specimen is 180×200×1300mm. The concrete cover was 30mm from bottom of cross section based on British Standard. The centre section of beam is a semi-circle shape. This is because of preventing stress concentration which may make unexpected crack when the flexural bonding is act to the specimen. The ultimate strain of concrete was 28MPa after curing age of 28days. The steel rebar used in this study has the yield strength of 300MPa and the nominal diameter of 9.53mm. In the case of the test variables, the embedment length of $5d_b$, $10d_b$, and $15d_b$ were considered based on the pure pull-out test of the GFRP rebar (Sim, 2004). The d_b means the nominal diameter of the steel and GFRP rebar. Figure 2 shows the detail of test specimen. The bonding length was defined from the end of semi-circle. And PVC pipe was installed on the unbonding section of the test beam and sealed at the both end of unbonding section of steel and GFRP rebar. The loading position was considered from the end of semi-circle to make sure the flexural bonding behavior effectively. Table 1 summarizes the test variables in this study.

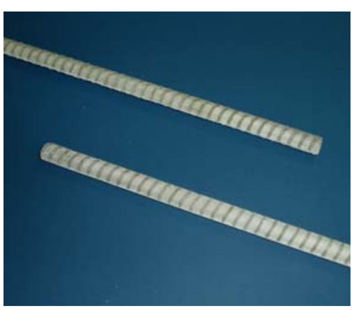

Figure 1. Newly-developed GFRP rebar.

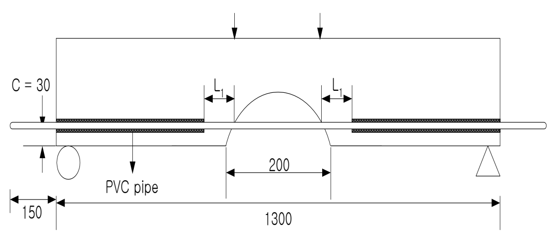

Figure 2.(a) 5 d_b specimen

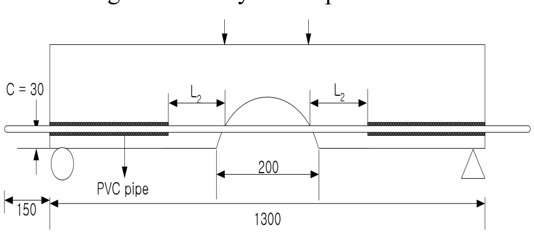

Figure 2.(b) 10 d_b specimen

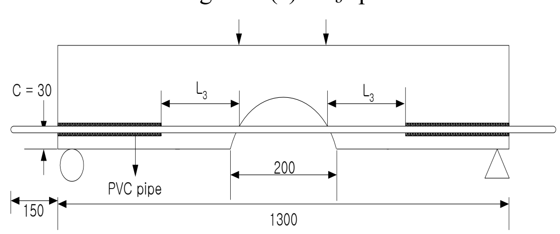

Figure 2.(c)15 d_b specimen

Figure 2. The experimental variables

Table 1. Summary of the test variables

Specimen	Reinforcing material	Embedment length (mm)	
$5d_b$	Steel	L_1	47.6
	GFRP		
$10d_b$	Steel	L_2	95.3
	GFRP		
$15d_b$	Steel	L_3	142.9
	GFRP		

Test Setup

Figure 3 shows the test setup in this study. As it commented before, four point bending test was performed with simply support in the each end of specimens. The loading test was performed by actuator with a capacity of 25kN. At this time, LVDT was installed at the end of left and right side of the test beam for measuring the load-slip relationship (see Figure 4). The LVDT was tightly fixed on the both end of rebar by using tied band. Loading step was 1mm/min subjected to the displacement control during the test. And all of experimental data were measured by automated data acquisition system. For fatigue test, the maximum and minimum stress level based on the portion of ultimate load for static test was considered.

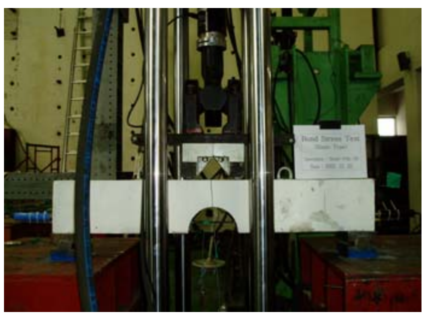

Figure 3. The test setup

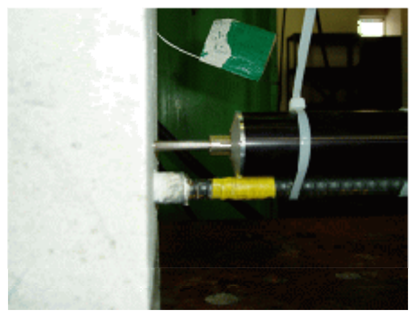

Figure 4. Measurement of slip of each reinforcement

Failure Pattern

Figures 6 - 7 show the test result of flexural bonding test for GFRP specimen. In the case of steel specimen, it had a similar failure mode with GFRP specimen. In the result of the test, generally, two failure modes were shown in this study: pull-out and concrete tensile failure. Among the three types of specimens, $5d_b$ specimen mainly showed pull-out failure and $15d_b$ specimen was subjected to concrete tensile failure. For $10d_b$ specimen, however, it had both pull-out and concrete tensile failure. In the case of $5d_b$ specimen, it has initial crack at the middle of beam with the crack load of 10kN. Figure 7 shows the pull-out failure of $5d_b$ specimen. The pull-out failure was preceded increasing the crack width at the middle of specimen. In the case of the surface of GFRP rebar, the ribs on the surface had any no defect when the pull-out failure occurs.

Figures 8 - 9 show the test result of flexural bonding test for $15d_b$ GFRP specimen. In this specimen case, all of specimen showed the concrete tensile failure. Crack initiated at the end of PVC pipe which is already installed as the unbonding section. For steel rebar reinforced specimen, it showed a similar failure shape to that of GFRP specimen. $15d_b$ GFRP specimen mainly failed as concrete tensile failure because the concrete could not afford to resist tensile stress which was act between bonded and unbonded section. And also any no defect on the surface of GFRP rebar was shown and slip value was less than that of steel reinforced specimen.

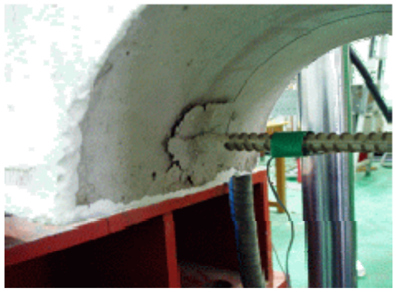

Figure 6. Pull-out failure.

Figure 7. Detail of Pull-out failure.

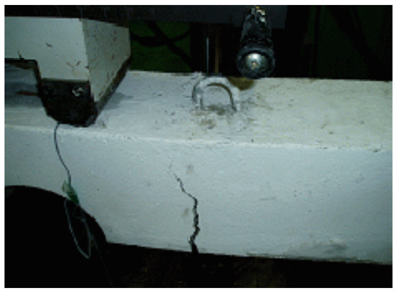

Figure 8. Concrete tensile failure

Figure 9. Detail view of bonded and unbonded section

Evaluation of Maximum Bonding Strength

Figure 10 shows maximum bonding strength of the test specimen. From this analysis result, it can be concluded that as the embedment length increase, the average bond strength diminishes and the specimens with shorter embedment length develop higher bond strength. $10d_b$ and $15d_b$ specimen, however, it was investigated that the failure was not pull-out failure but concrete tensile failure. Therefore, if concrete has enough tensile strength to prevent the concrete tensile failure, the bonding strength can be predicted as higher than that of concrete tensile failure. Figure 11 shows the embedment length – slip relationship. As the Figure notices, the GFRP specimen has less than slips of 0.3mm at the ultimate loading condition. In the case of steel bonding specimen, however, it shows as 0.4 to 1.5mm. Therefore, it can be verified that the GFRP specimen has more efficient resistance for slip than that of steel specimen even if it has larger vertical displacement than the steel bonding specimen until ultimate load condition. This is because the newly-developed rib of GFRP rebar acted effective bonding performance to the concrete.

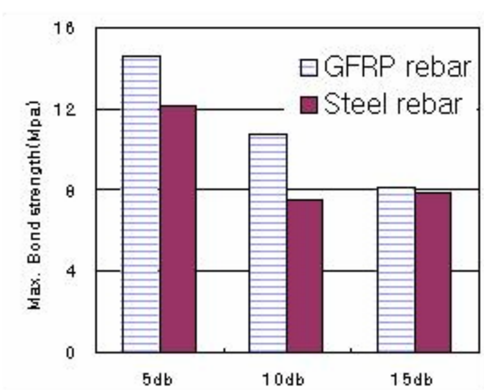

Figure 10. Maximum bond strength of the steel and GFRP specimen

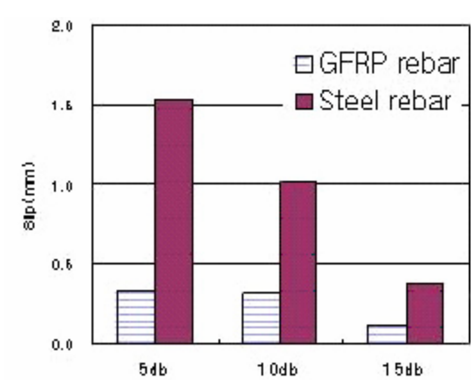

Figure 11. Comparisons of slip for the steel and GFRP specimen

Table 2 shows the summary of the result of static test. Test result showed that the same test specimen had similar ultimate loads with reasonable standard deviation. In the case of $5d_b$ specimen, all of test specimen showed pull-out failure. $5d_b$ GFRP specimen showed more 20% ultimate load than that of $5d_b$ steel specimen. Vertical deflection and slip, however, was less than that of $5d_b$ steel specimen. For $10d_b$ specimen, all of steel rebar specimen showed pull-out failure, however, GFRP specimen showed pull-out and concrete tensile failure. Vertical deflection and slip has a similar behavior to the $5d_b$ specimens. Lastly, all of $15d_b$ specimen showed concrete tensile failure.

Table 2. Summary of the result of static test.

Specimen	Analyzing index	Steel rebar No. 1	Steel rebar No. 2	GFRP rebar No. 1	GFRP rebar No. 2
$5d_b$	Ultimate load(kN)	10.9	10.0	12.9	11.9
	Vertical deflection(mm)	3.3	4.1	4.9	3.8
	Slip(mm)	1.3	1.7	0.4	0.3
	Failure mode	P/O*	P/O	P/O	P/O
	Maximum bonding strength(MPa)	12.8	11.7	15.1	14.0
$10d_b$	Ultimate load(kN)	-	16.6	17.4	19.3
	Vertical deflection(mm)	2.3	3.8	5.1	5.23
	Slip(mm)	0.8	1.2	0.3	0.3
	Failure mode	P/O	P/O	P/O	C/ T
	Maximum bonding strength(MPa)	5.3	9.8	10.2	11.3
$15d_b$	Ultimate load(kN)	20.6	19.6	22.7	19.1
	Vertical deflection(mm)	2.8	2.9	-	5.5
	Slip(mm)	0.2	0.5	0.1	0.1
	Failure mode	C/T**	C/ T	C/ T	C/ T
	Maximum bonding strength(MPa)	8.1	7.7	8.9	7.5

* Pull-out failure, ** Concrete tensile failure

Fatigue Test

Failure Pattern

The failure pattern of fatigue test was almost similar to that of static test. In the result of the fatigue test, generally, two failure modes were also shown in this study: pull-out and concrete tensile failure. Among the three types of specimens, $5d_b$ GFRP specimen showed pull-out failure and $15d_b$ GFRP specimen was subjected to concrete tensile failure. This fact can be considered that the embedment length of $15d_b$ GFRP specimen had an effective flexural bonding length to the concrete structure member with the compressive strength.

Table 3 shows the summary of the fatigue test. The fatigue test was controlled until failure loading number of 2,000,000 as the fatigue limit. As the Table 3 shows, all of stress level of 60%, 70% had the fatigue limit of 2,000,000 until failure. As the stress level increased until failure, the number of fatigue load decreased. And also, as the embedment length increased, the number of fatigue load increased too. This is because the longer embedment length makes the stress distribution well.

Table 3. Summary of the result of fatigue test

Specimen	Stress level (%)	No. of fatigue load	Failure mode
$5d_b$ GFRP	60	2,000,000	P/O
	70	2,000,000	P/O
	75	1,516,231	P/O
	80	29,268	P/O
$10d_b$ GFRP	70	2,000,000	C/T
	80	81,064	C/T
$15d_b$ GFRP	60	2,000,000	C/T
	70	2,000,000	C/T
	75	1,981,582	C/T
	80	193,972	C/T

Bond Stress-Slip Relationship

Figures 12 - 13 show the bond stress-slip relationship of $5d_b$ GFRP specimen with the result of static test. The relationship of the $15d_b$ GFRP specimen was not being considered in this time because the $5d_b$ specimen showed the pull-out failure which can be considered as a slip failure of the GFRP rebar. In the case of $5d_b$ GFRP 70% specimen which has the stress level of 70%, is showed fatigue limit of 2,000,000. And also the slip at the fatigue limit of 2,000,000 did not approach the ultimate slip of static test. This can be explained that the stress level of 70% is not a critical failure load at the fatigue behavior of the $5d_b$ GFRP specimen. For Figure 15, it illustrates the result of the fatigue behavior of $5d_b$ GFRP 75% specimen. The $5d_b$ GFRP 75% specimen showed the fatigue limit of 1,516,231 then it can be concluded the stress level of 75% is almost fatigue limit to the fatigue failure. Figures 14 - 15 show a similar fatigue behavior with around of the slip value as 0.25. From this test result, it can be evaluated that the ultimate slip of fatigue test approaches the critical slip at the static test increasing the stress level

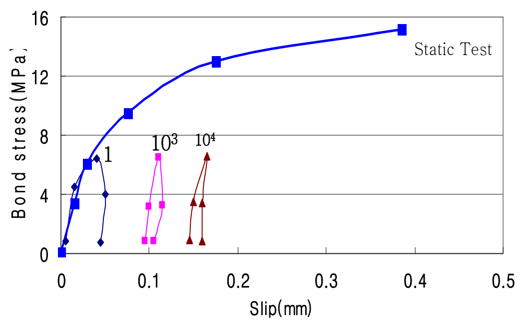

Figure 12.Bond stress – slip relationship of $5d_b$ GFRP 80% specimen

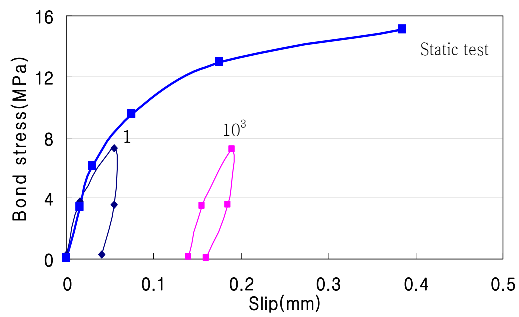

Figure 13. Bond stress – slip relationship of $5d_b$ GFRP 90% specimen

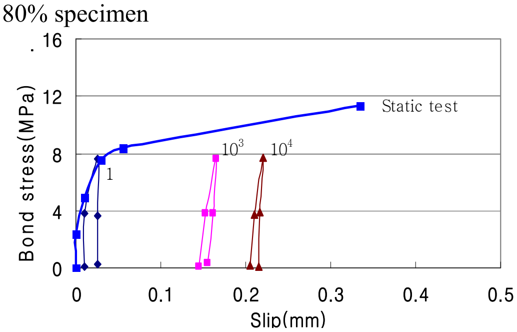

Figure 14. Bonds stress – slip relationship of $15d_b$ GFRP 80% specimen

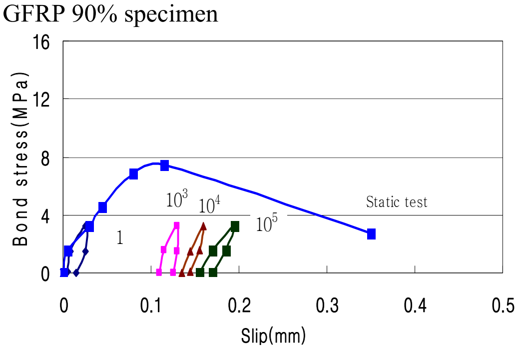

Figure 15. Bonds stress – slip relationship of $15d_b$ GFRP 80% specimen

S-N Relationship

Figure 16 shows the S-N relationship of GFRP specimen according to the stress level and No. of fatigue load in this study. The $5d_b$ specimen and $15d_b$ specimen is the representative of pull-out and concrete splitting failure, respectively. This relationship can be acquired by using regressive technique with the result of fatigue test. It is also based on the Miner theory. The Table 4 shows the result of the regressive procedures. The number of fatigue load conventionally expressed by Ln log function.

In the result of fatigue analysis, the fatigue limit of the GFRP rebar could be around of the stress level of 70%. This value means that the flexural bonding characteristics of the GFRP rebar will satisfy the service life of a concrete structure reinforced with the GFRP rebar.

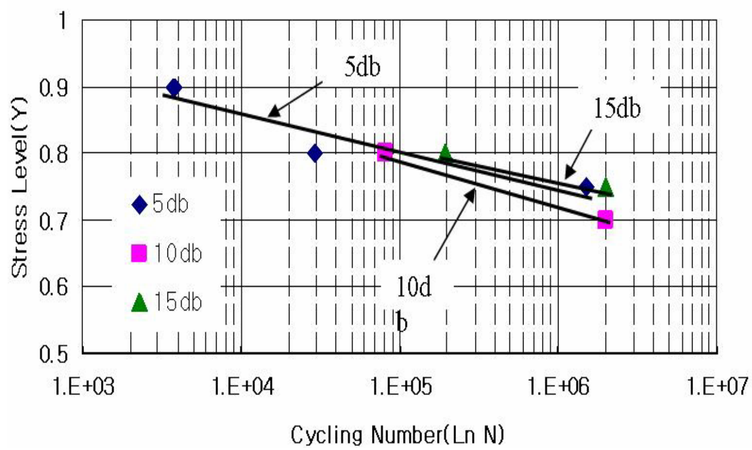

Figure 16. S-N relationship

Table 4. The result of fatigue life

Specimen	Fatigue life
$5d_b$	Y= -0.01891ln(N)+0.996
$10d_b$	Y= -0.0312ln(N)+1.1526
$15d_b$	Y= -0.0323ln(N)+1.193

CONCLUSIONS

The conclusions acquired by this experimental study are as follows.

In this study, the GFRP rebar was newly developed then the mechanical performance such as tensile strength was evaluated well. And also the flexural bonding test was performed to evaluate the flexural bonding capacity the GFRP rebar by using flexural concrete specimen. The flexural bonding characteristic of the GFRP rebar showed more effective than that of the conventional steel rebar from the result of the ultimate load – slip behavior.

In the case of the embedment length – slip relationship, the GFRP specimen has less slip than that of the steel specimen at the ultimate load. Therefore, it can be verified that the GFRP specimen has more efficient resistance for slip than that of steel specimen even though it has larger vertical deflection than the steel specimen until ultimate load. This is because the newly-developed rib of GFRP rebar acted effective bonding performance to the concrete.

In the result of fatigue test, the specimens which have the stress level of 60%, 70% showed the fatigue limit of 2,000,000 until failure. Especially, as the stress level increased until failure, the number of fatigue load decreased. And also, as the embedment length increased, the number of fatigue load increased too. Therefore, it was evaluated that the longer embedment length makes the stress distribution well.

For the S-N relationship, the fatigue limit of the GFRP rebar could be around of the stress level of 70%. This value means that the flexural bonding characteristics of the GFRP rebar will satisfy the service life of a concrete structure reinforced with the GFRP rebar. But in future, the fatigue life of the flexural bonding behavior for the GFRP rebar can be modified and improved with more experimental data.

This study evaluated the flexural bonding characteristics of the GFRP rebar. In the result of the test, the newly-developed GFRP rebar can be available to the structural design and analysis of concrete beam reinforced with the GFRP rebar in future.

ACKNOWLEDGEMENT

This research was partially supported by subsidiary research grant given to Korea Concrete Institute from 2005 Construction Core Technology Program D11, "Center for Concrete Korea" from the Ministry of Construction and Transportation. The financial support is gratefully acknowledged.

REFERENCES

British Standard (2000). *Determination of the bond behavior between reinforcing steel and autoclaved aerated concrete by the "beam test"*, The European standard IN 12269-1, 9.

Cosenza, E., Manfredi, G., Peace, M. and Realfonzo, R. (1995). "Analytical modelling of bond between FRP reinforcing bars and concrete", *Proceeding of 2nd International RILEM Symp(FRPRCS-2).*

Elighausen, R., Popov, E. P. and Bertero, V. V. (1983). "Local bond stress-slip relationships of deformed bars under generalized excitations", *Earthquake Engrg. Res. Ctr.(EERC),* Univ. of California, Berkeley, Calif No.2, 83-23.

Focacci, F., Nanni, A. and Bakis, C. E. (2004). "Local bond-slip relationship for FRP reinforcement in concrete", *Journal of composites for construction*, Vol.2, No.1, 24-31.

Park, J.S., You, Y.C., Park, Y.H., Choi, K.S., Kim, H.Y. and Kim, K.H. (2006). "An Experimental Study on the Bond Characteristics of Glass Fiber Reinforced Polymer Rebar", *Proceeding of the Korea Concrete Institute,* 16(1), 124-127.

Sim, J. (2004). *Development of smart and self-monitoring system for concrete structures using Hybrid FRR Rod*, Hanyang University, South Korea.

Tighiouart, B., Benmokrane, B., and Gao, D. (1998). "Investigation of bond in concrete member with fibre reinforced polymer (FRP) bars", *Construction and building materials,* 12, 453-462.